# Mathematical Modeling of a Renewable Energy-Connected PEM Water Electrolyzer

D.D. Hapuarachchi
*Department of Mechanical Engineering*
Faculty of Engineering, University of Sri Jayewardenepura
Rathmalana, Sri Lanka
damithadasun@gmail.com

H.G.S. Rangana
*Department of Mechanical Engineering*
Faculty of Engineering, University of Sri Jayewardenepura
Rathmalana, Sri Lanka
supunrangana@sjp.ac.lk

U.E. Thilakarathne
*Department of Mechanical Engineering*
Faculty of Engineering, University of Sri Jayewardenepura
Rathmalana, Sri Lanka
uvinduthilakarathne@sjp.ac.lk

I.U. Dedigama
*Department of Mechanical Engineering*
Faculty of Engineering, University of Sri Jayewardenepura
Rathmalana, Sri Lanka
ishankadedigama@sjp.ac.lk

*Abstract*— **This study provides the framework for optimizing a renewable energy-connected PEM electrolyzer. PEM electrolyzer was primarily enforced onto the electrolyzer process and different electrolyzers. The Key factors that need to be considered for the electrolyzer modeling process such as basic principles, modeling equations, and stack structure. There are several coupling technologies between solar PV and electrolyzers, such as direct coupling, coupling via an electronic converter, and battery-assisted electrolyzer. A mathematical model of solar PV-connected PEM electrolyzer is developed in this project. Then the mathematical model is optimized using optimizing parameters such as the temperature of solar PV, and the Operating temperature of the PEM electrolyzer of the PEM electrolyzer.**

***Keywords—PEM electrolyzer, solar PV generation, coupling between solar PV and electrolyzer, mathematical modeling, and model optimization.***

## I. INTRODUCTION

The world faces an energy crisis driven by depleting fossil fuels and escalating environmental damage. To combat these challenges, there is a shift towards renewable energy technologies. Since hydrogen does not exist naturally in its elemental or molecular form, it must be produced. Water, which contains hydrogen, is a readily available source for hydrogen production. Water electrolysis is the primary method used for splitting water molecules to generate hydrogen [1]. This research investigates the generation of green hydrogen using renewable energy, focusing on efficient energy conversion via fuel cells. Solar power, which is abundant in Sri Lanka, has been selected as the renewable energy source. The study explores the integration of Proton Exchange Membrane (PEM) water electrolysis (PEMWE) with solar photovoltaic (PV) technologies. A mathematical model of a PEM electrolyzer integrated with solar PV cells is developed, analyzing internal losses in PEMWEs and the effects of solar power integration on the electrolysis process. The goal is to establish a framework for optimizing solar PV-integrated PEMWEs.

## II. FUNDAMENTALS OF PEM ELECTROLYZER

### A. Basic principles

The splitting of water into oxygen and hydrogen, driven by electricity, is the core reaction in PEMWE. The Proton exchange membrane (PEM) is active as the electrolyte [1].

$$2\,H_2O_{(l)} \rightarrow 2\,H_{2(g)} + O_{2(g)} \qquad (1)$$

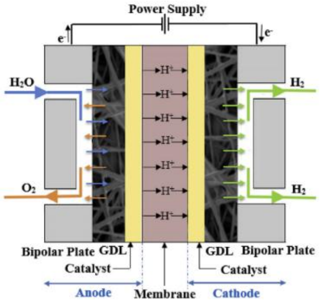

Figure 1: Schematic view of the PEM electrolyzer [2].

The key function of the membrane is that it only allows protons to pass through but not the electrons. A PEMWE consists of a proton exchange membrane, bipolar plates (BPs), gas diffusion layers (GDLs), and electrocatalysts of anode and cathode [1]. The chemical reactions at the anode and cathode;

$$\text{Anode}\ :\ 2\,H_2O_{(l)} \rightarrow 4H^+ + O_{2(g)} + 4e^- \qquad (2)$$

$$\text{Cathode:}\ 4H^+ + 4e^- \rightarrow\ 2\,H_{2(g)} \qquad (3)$$

### B. Stack structure of PEM electrolyzer

Originally, PEMWEs were made of expensive noble metal electrocatalysts and construction materials. The key reason for using such high-cost materials was the highly corrosive acidic environment PEM electrolyzers operated. Therefore, titanium stack components, noble metal electrocatalysts, and costly Nafion-type membranes were used for the construction of a PEMWE. PEMWE performance and cost have been improved over time. The following sections elaborate on the main components of the PEMWE such as BPs, GDLs, Proton exchange membrane, and the electrocatalysts layers and their functions.

## III. RENEWABLE ENERGY

Green hydrogen production is possible by integrating a PEMWE with renewable energy sources such as solar and wind. Combining solar and wind energy offers significant advantages, including supporting high peak demand, shifting grid loads to low-demand periods, and smoothing power fluctuations from variable renewable inputs. Solar energy is particularly prominent in Sri Lanka's renewable energy mix, especially for domestic power generation. This study focuses on using solar energy to power PEMWEs, with the potential to incorporate wind energy if required [3].

### *A. Solar Power Generation*

Solar energy can be harnessed through two primary methods: Concentrated Solar Power (CSP) and Photovoltaic (PV) systems. CSP systems convert thermal energy to electricity using reflectors and offer energy storage options, making them better suited for grid integration despite their high costs. PV systems, on the other hand, generate direct current (DC) electricity through the photovoltaic effect. While cost-effective, PV systems lack thermal energy production or storage capabilities [4].

### *B. Integration Between Solar PV and Electrolyzer*

Solar PV can be integrated with PEMWEs through three coupling methods: direct coupling, electronic converters, or battery-assisted systems. In a direct-coupling system, the PV array connects directly to the electrolyzer via DC. This method is simple, cost-effective for small-scale systems, and works well when both components are physically close. However, it suffers from power compatibility issues and is not suitable for larger setups. Using an electronic converter to couple the systems allows the PV and electrolyzer to operate independently at their optimal power points. This setup is adaptable for co-located or distant systems, utilizing either high-voltage DC transmission or traditional AC systems with conversion stages.

Battery-assisted electrolyzers address the variability of solar-powered electrolysis by smoothing hydrogen production and extending operational periods. Although this method is costly, it improves system reliability by providing backup energy. Batteries can support the electrolyzer during low PV output, maintain consistent operation at fixed power levels, or adjust the operating point based on seasonal or daily variations [5].

### *C. Solar Power Impact*

The efficiency of solar power generation depends on solar irradiance, panel efficiency, and the tilt angle of PV panels. Proper optimization of tilt angles ensures maximum energy generation and minimizes mismatches between solar power output and hydrogen production, enhancing the overall performance of PV-assisted PEMWE systems [6].

## IV. METHODOLOGY

At the outset of this study, a comprehensive literature review was conducted to understand the principles and associated losses of PEMWEs, solar PV systems, methods for integrating the two, model development techniques, and optimization processes. A mathematical model of a PEMWE was developed using MATLAB to analyze the effects of internal losses and operating parameters on electrolyzer performance. Solar PV polarization curves were obtained from PVSYST software and incorporated into a solar PV-connected electrolyzer model to determine hydrogen production rates based on solar irradiance in Colombo. The study considered solar panels with an 80 W capacity, necessitating a PEMWE system of equivalent or greater capacity. A PEMWE stack comprising two cells with a combined capacity of 80 W was integrated with the solar PV system. An ideal DC/DC buck converter was employed to connect the solar PV system to the PEMWE. The mathematical model was optimized by varying operating parameters, including the temperature of the solar PV panels and the temperature and pressure of the PEMWE. Further optimization involved incorporating a backup battery to enhance the performance of the solar PV-connected electrolyzer system.

## V. MATHEMATICAL MODEL

### *A. Assumptions*

The model shown here is based on the following simplified assumptions: The steady-state parameters include a constant temperature (25 °C) and air pressure (1 atm), perfect gases, 100% Faradaic efficiency, fully hydrated membrane, and no gas cross-over. The current across the cell is assumed to be evenly distributed.

$$i = \frac{I}{A} \tag{4}$$

Where $I$ is the current, $i$ is the current density and $A$ is the active area.

The physical parameters and materials of construction of the PEMWE were assumed based on the literature survey conducted and are tabulated in Tables 1 and 2.

Table 1: Materials of the PEM Electrolyzer

| **Component** | **Material** |
|---|---|
| Membrane | Nafion |
| Anode/Cathode electrode | Platinum |
| Anode GDL | Titanium (Platinum coated) |
| Cathode GDL | Toray carbon paper |
| Bipolar plate | Titanium |

Table 2: Physical parameter of the PEM electrolyzer

| **Parameter** | **Value** | **Parameter** | **Value** |
|---|---|---|---|
| $T$ | $298\,K$ | $w_{s,an}$ | $3.6\,mm$ |
| $P$ | $1\,atm$ | $w_{s,cat}$ | $1.0\,mm$ |
| $A$ | $10\,cm^2$ | $h_{p,an}$ | $12\,mm$ |
| $\delta_m$ | $0.178\,mm$ | $h_{p,cat}$ | $11.7\,mm$ |
| $\delta_{an}$ | $5 \times 10^{-2}\,mm$ | $h_{c,an}$ | $3.0\,mm$ |
| $\delta_{cat}$ | $5 \times 10^{-2}\,mm$ | $h_{c,cat}$ | $1.0\,mm$ |
| $L$ | $20\,mm$ | $n_{c,an}$ | 9 |
| $W$ | $50\,mm$ | $n_{c,cat}$ | 30 |
| $w_{c,an}$ | $2.5\,mm$ | $n_{s,an}$ | 8 |
| $w_{c,cat}$ | $1.0\,mm$ | $n_{s,cat}$ | 30 |

Table 3: Estimated parameter values

| **Parameter** | **Value** |
|---|---|
| $\alpha_{an}$ | 2 [7] |
| $\alpha_{cat}$ | 1 [8] |
| $D_w$ | $1.28 \times 10^{-10}\ m^2 s^{-1}$ [9] |
| $\varepsilon$ | 0.3 [9] |
| $a_{H_2O}$ | 1 [10] |
| $i_{0,an}$ | $3 \times 10^{-6}\ A\ cm^{-2}$ [9] |
| $i_{0,cat}$ | $2.3 \times 10^{-3}\ A\ cm^{-2}$ [10] |
| $C_{H^+}$ | $1200\ mol\ m^{-3}$ [9] |
| $D_{H^+}$ | $4.5 \times 10^{-9}\ m^2 s^{-1}$ [9] |
| $\rho_{el}$ | $9.85 \times 10^{-8}\ \Omega$ m [9] |
| $\rho_{an}$ | $47.8 \times 10^{-8}\ \Omega$ m [9] |
| $\rho_{cat}$ | $16 \times 10^{-8}\ \Omega$ m [9] |
| $P_{sat}$ | $0.467 atm$ [9] |
| $M_{m,dry}$ | $1.1\ kg\ mol^{-1}$ [9] |
| $\rho_{m,dry}$ | $2000\ kg\ m^{-3}$ [9] |

### B. Mass balance

A PEM electrolyzer's mass balancing entails measuring the flow of reactants and products to ensure mass conservation throughout the electrochemical process of hydrogen generation.

$$\dot{m}_{H_2O,out,an} = \dot{m}_{H_2O,in} - \dot{m}_{H_2O,mem} - \dot{m}_{H_2O,cons} \quad (5)$$

$$\dot{m}_{H_2O,out,cat} = \dot{m}_{H_2O,mem} \quad (6)$$

$$\dot{m}_{H_2O,mem} = \dot{m}_{H_2O,dd} + \dot{m}_{H_2O,eo} \quad (7)$$

Where $\dot{m}_{H_2O,out,an}$ is the outlet mass flow rate of water at the anode, $\dot{m}_{H_2O,out,cat}$ is the outlet mass flow rate of water at the cathode, $\dot{m}_{H_2O,in}$ is the inlet mass flow rate of water at the anode, $\dot{m}_{H_2O,mem}$ is the mass flow rate of water through the membrane, $\dot{m}_{H_2O,cons}$ is the mass flow rate of water consumed by the electrochemical reaction split into $H_2$ and $O_2$, $\dot{m}_{H_2O,dd}$ is the mass flow rate of water flowing from anode to cathode due to the concentration gradient and $\dot{m}_{H_2O,eo}$ is the mass flow rate of water due to the concentration of electro-osmotic drag. Molar flow rate of species $i$ can be related to its mass flow rate;

$$\dot{N}_i = \frac{\dot{m}_i}{M_i} \quad (8)$$

Where $\dot{m}_i$ is the mass flow rate of species, $M_i$ is the molar mass of species and $\dot{N}_i$ is the molar flow rate of species.

Faraday's law relates the molar flow rates of hydrogen and oxygen production, as well as water consumption, to the cell current and is given by,

$$\dot{N}_{H_2} = \frac{I}{2F}, \qquad \dot{n}_{H_2} = \frac{i}{2F} \quad (9)$$

$$\dot{N}_{O_2} = \frac{I}{4F}, \qquad \dot{n}_{O_2} = \frac{i}{4F} \quad (10)$$

$$\dot{N}_{H_2O,cons} = \frac{I}{2F}, \qquad \dot{n}_{H_2O,cons} = \frac{i}{2F} \quad (11)$$

Where $\dot{n}$ is the molar flux and $F$ is the Faraday constant (96485 $C\ mol^{-1}$).

### C. Diffusion transport

In the PEM electrolyzer, water diffusion through the membrane is caused as a result of the difference in water concentration across the membrane. A constant supply of water across the anode forces the water to flow from the anode to cathode. Assuming there is water circulation only on the anode side, the cathode can expected to be dry at the beginning of electrolysis creating a large concentration gradient [9].

$$\dot{N}_{H_2O,dd} = \frac{AD_{eff}}{\delta_m}\left(C_{H_2O,an} - C_{H_2O,cat}\right) \quad (12)$$

$$D_{eff} = \varepsilon^{1.5} D_w \quad (13)$$

Where $C_{O_2,mem}$ is the oxygen concentration at the membrane electrode interface, $C_{H_2,mem}$ is the hydrogen concentration at the membrane electrode interface, $C_{O_2,0}$ is the Oxygen reference concentration, $C_{H_2,0}$ the Hydrogen reference concentration and $D_{eff}$ is the effective water diffusion coefficient in the membrane.

### D. Electro-osmotic drag

Electro-osmotic drag is caused by to flux of hydrogen protons that are moving between electrodes. Hydrogen protons drag water molecules along with them. As a result, water transports from anode to the cathode [9],[11].

$$\dot{N}_{H_2O,eo} = \frac{n_{drag}\, I}{F} \quad (14)$$

$$n_{drag} = 0.03 + 0.0134\, T \quad (15)$$

Where $n_{drag}$ is the electro-osmotic drag coefficient and $T$ is the temperature.

### E. Voltage

The overall performance of a PEMWE can be determined through a polarization curve. It indicates the relationship between the current/current density and the voltage. In a single PEMWE, the total potential is a combination of open circuit voltage, activation overpotential, diffusion overpotential, and ohmic losses [7],[12].

$$V_{cell} = E + \eta_{act} + \eta_{dd} + \eta_{ohm} \quad (16)$$

Where $V_{cell}$ is the cell voltage, $E$ is Open circuit voltage, $\eta_{act}$ is the activation overpotential, $\eta_{dd}$ is diffusion or concentration overpotential $\eta_{ohm}$ is ohmic overpotential.

Open circuit voltage

#### 1) Open circuit voltage

Open circuit voltage is the theoretical minimum voltage of a PEMWE when other overpotentials are neglected. The open circuit voltage is usually determined using the Nernst equation [7][12].

$$E = E^0 + \frac{RT}{2F} \ln\left(\frac{P_{H_2}\sqrt{P_{O_2}}}{a_{H_2O}}\right) \quad (17)$$

Where $E^0$ is the equilibrium cell voltage at standard conditions, $P_{H_2}$ is the partial pressure of hydrogen, $P_{O_2}$ is the partial pressure of oxygen, $a_{H_2O}$ is the activity of water and $R$ is the universal gas constant($8.314\ J\ mol^{-1}\ K^{-1}$). The equilibrium cell voltage can be determined using the equation below.

$$E^0 = 1.229 - 0.9 \times 10^{-3}(T - 298) \quad (18)$$

#### 2) Activation overpotential

At the electrode surfaces, activation losses relate to the electrochemical kinetic behavior of the electrochemical processes. They relate to the speed of reactions taking place at the electrode surfaces, therefore, these losses are induced due to the portion of voltage lost transferring electrons to or from the electrodes [7],[12]. This overpotential can be determined using the Butler-Volmer equation,

$$\eta_{act,an} = \frac{RT}{\alpha_{an}F}\ln\left(\frac{i}{i_{0,an}}\right) \quad (19)$$

$$\eta_{act,cat} = \frac{RT}{\alpha_{cat}F}\ln\left(\frac{i}{i_{0,cat}}\right) \quad (20)$$

Where $\alpha_{an}$ is the charge transfer coefficient at the anode, $\alpha_{cat}$ is the charge transfer coefficient at the cathode, $i_{0,cat}$ is the cathode exchange current density and $i_{0,an}$ is the anode exchange current density.

Activation overpotential can be determined by taking the addition of anode activation overpotential and cathode activation overpotential,

$$\eta_{act} = \eta_{act,an} + \eta_{act,cat} \quad (21)$$

### 3) *Diffusion overpotential*

Diffusion overpotential is caused due to the mass transport that happens inside the porous electrodes of PEMWEs. During the electrolysis process, mass transport significantly affects PEMWE due to the two-phase flow between liquid water transporting to the reaction layer and the gases being removed from the reaction sites [7],[12].

This overpotential can be determined by given equations;

$$\eta_{dd,an} = \frac{RT}{4F}\ln\left(\frac{C_{O_2,mem}}{C_{O_2,0}}\right) \quad (22)$$

$$\eta_{dd,cat} = \frac{RT}{2F}\ln\left(\frac{C_{H_2,mem}}{C_{H_2,0}}\right) \quad (23)$$

Where $C_{O_2,mem}$ oxygen concentration at the membrane electrode interface is, $C_{H_2,mem}$ is hydrogen concentration at the membrane electrode interface $C_{O_2,0}$ is oxygen reference concentration and $C_{H_2,0}$ is hydrogen reference concentration.

Diffusion overpotential can be determined taking addition of anode diffusion overpotential and cathode diffusion overpotential

$$\eta_{dd} = \eta_{dd,an} + \eta_{dd,cat} \quad (24)$$

### 4) *Ohmic overpotential*

Ohmic losses are generated due to resistivity that is induced when ions and electrons travel through the electrolyte and electrodes. The conductivity of the electrolyte and the materials used in electrodes and the membrane dictate these losses. The degree of ohmic losses depends on the characteristics of the material. The ohmic overpotential is directly correlated to the substance's resistance to proton flow [7],[12]. Ohmic overpotential depends on the current and the total resistance of the cell ($R_{cell}$).

$$\eta_{ohm} = R_{cell}I \quad (25)$$

The ohmic overpotential is mostly caused by resistance on the bipolar plate, electrodes, membranes, and interfacial layers. This relationship may be represented as follows [8]:

$$\eta_{ohm} = \eta_{ohm,el} + \eta_{ohm,p} + \eta_{ohm,m} \quad (26)$$

Where $\eta_{ohm,el}, \eta_{ohm,p}, \eta_{ohm,m}$ are the ohmic overpotentials caused by the electrodes, bipolar plates, and the membrane respectively.

## VI. RESULTS AND DISCUSSION

### A. *PEM electrolyzer*

The standard open circuit voltage ($E^0$) of the electrolyzer is calculated to be 1.229 V at a temperature of 298 K, while the modeled open circuit voltage (E) is determined as 1.435 V. The study also analyzed activation overpotentials, examining their behavior with increasing current density and their impact on overall cell performance.

The study reveals that activation overpotentials are more significant at lower current densities and decrease at higher current densities.

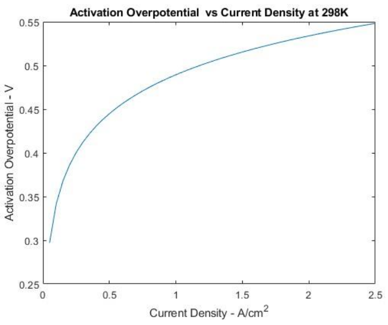

Figure 2: Current density vs. Activation overpotential.

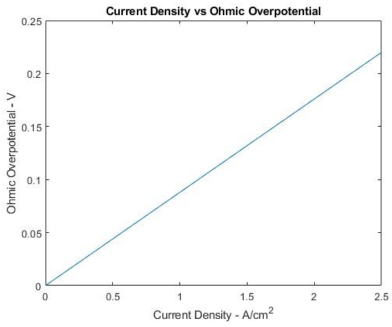

Figure 3: Current density vs. Ohmic overpotential.

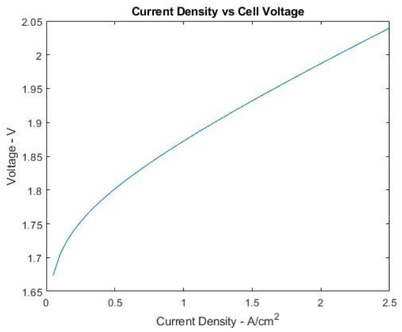

Figure 4: Current density vs. Cell voltage.

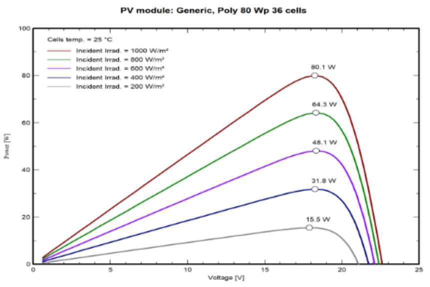

Figure 5: Power and Voltage of solar PV with irradiance.

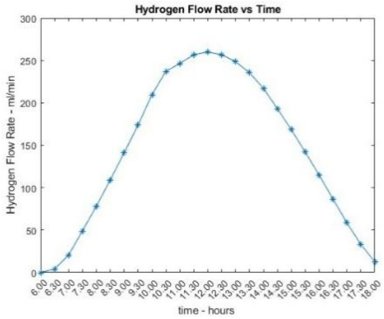

Figure 6: Hydrogen production rate vs. time

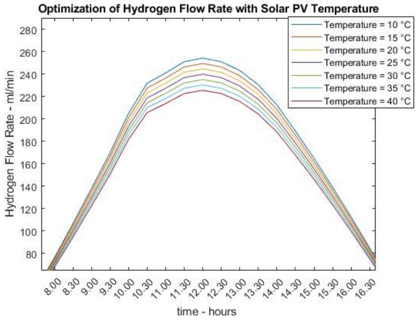

Figure 7: Hydrogen production rate with solar PV solar temperature

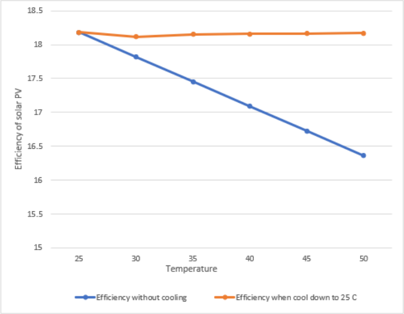

Figure 8: Solar PV temperature vs solar PV efficiency.

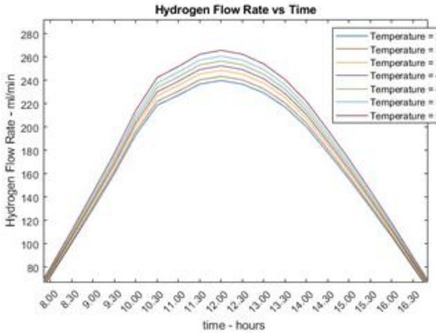

Figure 9: Hydrogen production optimizations with the temperature of the electrolyzer.

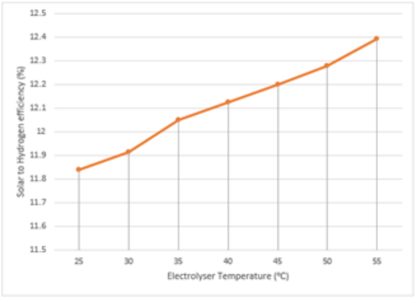

Figure 10: PEM Electrolyzer temperature vs solar to hydrogen efficiency.

Additionally, the cathode activation overpotential is negligible compared to the anode activation overpotential, indicating that the oxygen evolution reaction at the anode is the rate-determining step. The total activation overpotential is determined by combining the anode and cathode activation overpotentials.

### *1) Ohmic overpotential*

Resistance was determined separately for the bipolar plates, electrodes, and membranes. The ohmic overpotential of the PEMWE with increasing current density is shown in Figure 3. It can be seen that the ohmic overpotential increases linearly with increasing current density indicating it is proportional to the current density.

### *2) Concentration overpotential*

Concentration losses in PEMWE arise from mass transport issues caused by gas-blocking reactant flow to the electrode. However, with optimized flow fields for gas removal and consistent water circulation, these losses become negligible.

### *3) Cell Voltage*

Cell voltage is determined by combining the open circuit voltage, activation overpotential at the anode and cathode, and ohmic overpotential as shown in Figure 4. It shows the voltage and current density variation of a theoretical PEMWE. The 80 W PEMWE stack integrated with solar PV considered in this study is maintained at a single-cell voltage of 2 V giving the total stack voltage as 4 V. The polarization data shown in Figure 4 shows that the cells will operate a current density of 2.25 $Acm^{-2}$ at the voltage considered (2V).

## *B. Solar PV*

PV module- Poly 80 W 36 cells solar panel is considered to be connected to a PEMWE to generate hydrogen through electrolysis. The solar PV was analyzed using PVSYST software. It was observed that the output power of the solar PV depends on solar irradiance as shown in Figure 5. It can clearly be seen that the power output increases with solar irradiance.

## *C. Solar PV-connected PEM electrolyzer*

The study considers the connection between solar PV and PEMWE stack through a buck converter. It can step down the PV voltage to match the electrolyzer operating voltage. When the electrolyzer is connected to the solar PV, the hydrogen generation rate depends on the power generation rate of the solar PV which is directly proportional to the solar irradiance. Based on this relation, a solar PV-connected electrolyzer model was developed by using MATLAB. Solar irradiance in Colombo was used to develop the model. The model was used to determine the hydrogen production rate of the PEMWE stack during standard operation within a day as shown in Figure 6. The highest solar irradiance comes to the Earth at 12:00 PM giving the maximum hydrogen production rate at this time. Figure 6 shows the variation in hydrogen production rate with changing solar irradiance on a typical day in Colombo.

## *D. Model Optimization*

Solar PV-connected PEM electrolyzer model can be optimized using optimizing parameters that affect the hydrogen production rate of the PEMWE stack. In this project, the model is optimized using the temperature of the solar PV, electrolyzer operating temperature and pressure, and a combination of solar PV, PEMWE, and backup battery. It was discussed earlier that the hydrogen production rate increases with increasing solar PV power. However, Figure 7 shows that a decrease in the temperature of the solar PV increases the hydrogen production rate.

Figure 8 shows the variation of solar panel efficiency with changing panel temperature. It can be observed that maximum efficiency can be achieved by maintaining the panel temperature at ambient conditions. The overall system efficiency can be enhanced by maintaining the solar PV temperature. However, the power requirement to cool down the solar panels needs to be considered when optimizing the system. The increase in system efficiency with reduced panel temperatures should not be set off by the energy consumed for panel cooling. The PEMWE stack can be optimized with the operating temperature of the electrolyzer. Figure 9 shows that the increasing operating temperature of the stack increases the hydrogen production rate.

The stack operating temperature can be increased by heating the water. PEM electrolyzer efficiency can be enhanced by increasing the water temperature with the power requirement of the water heating process. Therefore, solar to hydrogen efficiency also increased. The optimum PEM electrolyzer operating temperature depends on the maximum operating temperature of the PEM electrolyzer. The graph below shows solar to hydrogen efficiency with electrolyzer operating temperature.

Solar PV-connected electrolyzer systems can be optimized using a backup battery. This system can be established with a larger solar panel that generates power greater than the PEMWE stack or using a separate dedicated panel for the battery performance. When using large solar PV, it can produce power to the stack and charge the battery during high solar irradiance. During lower solar irradiance, the battery can supply power to the stack. When using separate solar panels to charge the battery, the battery can supply power to stack during lower solar irradiance [13].

## VII. CONCLUSION

This research mainly focuses on developing and optimizing a mathematical model of a solar PV-connected PEMWE. In order to develop the model it was needed to understand and identify principles of solar power generation, PEM electrolyzer principles, operating parameters of PEM electrolyzer, and integration of solar PV and electrolyzer. The final achievement is optimizing the mathematical model of the PEM electrolyzer using optimizing parameters such as the operating temperature of the electrolyzer, the operating pressure of the electrolyzer, and the temperature of solar PV.

## VIII. REFERENCES

[1] K. Zhang *et al.*, “Status and perspectives of key materials for PEM electrolyzer,” *Nano Res. Energy*, vol. 1, no. 3, pp. 1–8, 2022, doi: 10.26599/NRE.2022.9120032.

[2] S. Toghyani, S. Fakhradini, E. Afshari, E. Baniasadi, M. Y. Abdollahzadeh Jamalabadi, and M. Safdari Shadloo, “Optimization of operating parameters of a polymer exchange membrane electrolyzer,” *Int. J. Hydrogen Energy*, vol. 44, no. 13, pp. 6403–6414, 2019, doi: 10.1016/j.ijhydene.2019.01.186.

[3] A. Zahedi, “Sustainable power supply using solar energy and wind power combined with energy storage,” *Energy Procedia*, vol. 52, pp. 642–650, 2014, doi: 10.1016/j.egypro.2014.07.120.

[4] K. N. Nwaigwe, P. Mutabilwa, and E. Dintwa, “An overview of solar power (PV systems) integration into electricity grids,” *Mater. Sci. Energy Technol.*, vol. 2, no. 3, pp. 629–633, 2019, doi: 10.1016/j.mset.2019.07.002.

[5] V. A. Martinez Lopez, H. Ziar, J. W. Haverkort, M. Zeman, and O. Isabella, “Dynamic operation of water electrolyzers: A review for applications in photovoltaic systems integration,” *Renew. Sustain. Energy Rev.*, vol. 182, no. September 2022, p. 113407, 2023, doi: 10.1016/j.rser.2023.113407.

[6] M. Chandrasekar, P. Gopal, C. Ramesh Kumar, and V. Edwin Geo, “Effect of solar photovoltaic and various photovoltaic air thermal systems on hydrogen generation by water electrolysis,” *Int. J. Hydrogen Energy*, vol. 47, no. 5, pp. 3211–3223, 2022, doi: 10.1016/j.ijhydene.2021.04.205.

[7] B. Han, S. M. Steen, J. Mo, and F. Y. Zhang, “Electrochemical performance modeling of a proton exchange membrane electrolyzer cell for hydrogen energy,” *Int. J. Hydrogen Energy*, vol. 40, no. 22, pp. 7006–7016, 2015, doi: 10.1016/j.ijhydene.2015.03.164.

[8] H. Zhang, S. Su, G. Lin, and J. Chen, “Efficiency calculation and configuration design of a PEM electrolyzer system for hydrogen production,” *Int. J. Electrochem. Sci.*, vol. 7, no. 5, pp. 4143–4157, 2012, doi: 10.1016/s1452-3981(23)19527-7.

[9] I. Dedigama, K. Ayers, P. R. Shearing, and D. J. L. Brett, “An Experimentally Validated Steady State Polymer Electrolyte Membrane Water Electrolyzer Model,” vol. 9, pp. 2662–2681, 2014.

[10] D. Hyun, M. Chung, J. Rubin, and T. Supervisor, “Techno-Economic Assessment of Electrolytic Hydrogen Production under Dynamic Operations,” 2022.

[11] N. Z. Dmitri Bessarabov, Haijiang Wang, Hui Li, *PEM Electrolysis for Hydrogen Production, Principles and Applications. Chapter 11: Degradation Processes and Failure Mechanisms in PEM Water Electrolyzers*, no. 9. 2016.

[12] A. M. F. R. Pinto, “A review on PEM electrolyzer modeling : Guidelines for beginners,” vol. 261, 2020, doi: 10.1016/j.jclepro.2020.121184.

[13] F. Report, “Optimizing an Integrated Solar- Electrolysis System Cooperative Research and Development Final Report NREL Technical Contact : Josh Eichman Optimizing an Integrated Solar- Electrolysis System Cooperative Research and Development Final Report NREL Technica,” no. July, 2020.

[14] S. Saikia, V. Verma, B. K. Kakati, T. Sivasakthivel, and R. Tarodiya, “Optimization of solar integrated electrolyzer system for hydrogen production using Taguchi method,” *Mater. Today Proc.*, vol. 49, no. xxxx, pp. 397–402, 2021, doi: 10.1016/j.matpr.2021.02.304.

[15] D. Ghribi, A. Khelifa, S. Diaf, and M. Belhamel, “Study of hydrogen production system by using PV solar energy and PEM electrolyzer in Algeria,” *Int. J. Hydrogen Energy*, vol. 38, no. 20, pp. 8480–8490, 2013, doi: 10.1016/j.ijhydene.2012.09.175.

[16] M. M. M. Elamari, “Optimisation of Photovoltaic-Powered Electrolysis for Hydrogen production for a remote area in Libya,” 2011.

[17] I. Dedigama *et al.*, “In situ diagnostic techniques for characterisation of polymer electrolyte membrane water electrolyzers - Flow visualisation and electrochemical impedance spectroscopy,” *Int. J. Hydrogen Energy*, vol. 39, no. 9, pp. 4468–4482, 2014, doi: 10.1016/j.ijhydene.2014.01.026.